Structure and magnetic properties of the high-T_c related phase Cm_2CuO_4

L. Soderholm, S. Skanthakumar, and C. W. Williams
Chemistry Division, Argonne National Laboratory, Argonne, Illinois 60439
(Received 18 March 1999)

Neutron-diffraction, x-ray absorption, and magnetic susceptibility measurements have been used to characterize the structural and magnetic properties in a 42-mg powder sample of Cm_2CuO_4. This curium compound crystallizes in the tetragonal $I4/mmm$ space group, and is isostructural with the R_2CuO_4 (R=Pr-Gd) series that become superconducting upon electron doping. The lattice parameters, Cm-O distance, x-ray-absorption edges, and magnetic susceptibility data indicate that the Cm is trivalent. The Cm spins order antiferromagnetically below 25 K, although the magnetic and chemical unit cells are identical. The spins, which order ferromagnetically within the a-b plane, are antiferromagnetically coupled along the c axis, that is, adjacent planes are coupled antiparallel along c. These results are discussed in terms of the absence of superconductivity in the Th-doped analog. [S0163-1829(99)05229-7]

INTRODUCTION

The R_2CuO_4 phases (R=La, Pr-Gd) are parent compounds for high-temperature superconductors. With the appropriate doping of trivalent La by holes (Sr^{2+}, Ba^{2+}) or of trivalent Pr-Eu by electrons (Ce^{4+}, Th^{4+}), the resulting solid solutions are superconductors with T_c's of 32 K (Ref. 1) and 24 K,[2] respectively. Although the La analog has an orthorhombic structure (*Cmca*) similar to the Pr-Eu series ($I4/mmm$),[13] these two structures differ in the location of one crystallographic oxygen. The La analog is also the only phase in this series that becomes a hole superconductor. Cm_2CuO_4 forms a single phase material that crystallizes in a structure consistent with $I4/mmm$ symmetry.[3] A cusp in the magnetic susceptibility as a function of temperature at 25 K indicates a magnetic ordering of the Cm moments. Doping with Th^{4+} to form $Cm_{2-x}Th_xCuO_4$ results in a single phase material for $x \approx 0.18$, but the sample is not superconducting. The purpose of the work described herein is to further characterize the structure, electronic, and magnetic properties of the parent compound Cm_2CuO_4.

There are several features about Cm_2CuO_4 that need clarification. First is its structure. Although trends in lattice constants indicate that Cm_2CuO_4 is isostructural with the so called T' phase of the Pr-Gd analogs, the structure needs to be experimentally determined. The introduction of either holes or electrons to produce superconductivity is dependent on the details of the oxygen distribution about Cu in this structure. In addition, it has been suggested that there are interstitial Cm or oxygen ions that influence the superconducting properties of these materials.[4] The second point that needs clarification is the valence of Cm. Cm is the actinide analog of Gd, with a trivalent ionic radius slightly smaller than Nd.[5] Cm has a reduction potential similar to Pr, which means that it can form either trivalent or tetravalent oxides.[6] In order to rule out significant charge transfer from Cm to Cu, it is necessary to directly determine the valence state of Cm in this material. The third point that needs clarification is the source of the cusp observed in the magnetic susceptibility at 25 K. Cm^{3+} has a f^7 configuration with a nominal $^8S_{7/2}$ ground state, which to first order is spherically symmetric and therefore should not be influenced by the symmetry of the crystal field. However, splittings as high as 40 cm^{-1} (57.2 K) have been reported for Cm^{3+}, where they have been attributed to the effects of intermediate coupling.[7] In contrast, intermediate coupling cannot split the Cm^{4+} ground state, which is a singlet ($J=0$). The cusp observed in the susceptibility could originate from the magnetic ordering of the Cm^{3+} spins, or it could be the result of charge transfer, structural changes or crystal-field effects. Clarifying these points should further the understanding of the synergism between magnetism and high-temperature superconductivity.

The experiments discussed herein have been undertaken using neutron diffraction, magnetic susceptibility, and x-ray-absorption spectroscopy. Neutron-diffraction data have been used to determine both the nuclear and magnetic structures of this compound. X-ray-absorption spectroscopy confirms the conclusions from diffraction and magnetic data that Cm is trivalent in this host.

EXPERIMENTS

^{248}Cm, atomic number 96, is a manmade, radioactive isotope ($t_{1/2}=3.5\times10^5$ years, 91% α, 8.26% spontaneous fission), available only in mg quantities (Cm must be handled and transported with appropriate safety protocols). A 42-mg powder sample of Cm_2CuO_4 was prepared by following procedures optimized for Pr_2CuO_4. The details of sample preparation can be found elsewhere.[3] Phase purity was checked by x-ray diffraction. X-ray powder patterns were obtained using a Scintag diffractometer operating with a copper tube, and in theta-theta geometry.

The magnetization experiments were conducted on a Quantum Design superconducting interference device (SQUID) under an applied magnetic field of 1000 G. The sample was doubly encapsulated in aluminum containers. The empty containers were run independently to determine the background correction to the data.

X-ray-absorption experiments were conducted on powder samples at room temperature on the BESSRC bending magnet beamline 12BM at the Advanced Photon Source (APS) at

the Argonne National Laboratory. Cm-, L_3, L_2, and L_1 edge data were collected with a Si (111) double-crystal monochromator that gives an energy resolution of $\Delta E/E = 14.1 \times 10^{-5}$. Literature values for these edge positions are reported at 18 930, 23 779, and 24 460 eV, respectively.[8] Harmonic rejection was accomplished using a Pt mirror, set to reject energies higher than 25 keV. The use of harmonic rejection at these energies is necessary at the APS because of the high flux of high-energy photons. The energy was calibrated by setting the inflection point of the first derivative from the Nb K edge to 18 989 eV. All data were taken in the fluorescence and transmission mode simultaneously, using a flow-type ion chamber (The EXAFS Co.) as a detector.[9] The detector was charged with xenon gas and used without slits or a scattered-radiation filter. This is a common approach with the conventional 45°-incident/45°-exit fluorescence XAFS configuration, which minimizes the scattered radiation to the detector. The method of data analysis is described elsewhere.[9]

Neutron-diffraction data were taken on this sample using the Special Environment Powder Diffractometer (SEPD) at the Intense Pulsed Neutron Source at Argonne National Laboratory. The sample was sealed in a vanadium sample holder and further masked with Cd to improve the background. Data were obtained at room temperature, 35 ± 3 K, and 15 ± 4 K using a closed-cycle refrigerator. Problems with the thermocouple placement and sample self-heating resulted in a relatively large error in the determination of the sample temperature. Each data set took approximately 48 h to collect. Neutron data were collected simultaneously at three different detector banks with an average angle of 150°, 90°, and 60°, which have resolution of $\Delta d/d = .0034$, 0.0054, and 0.0088, respectively. In order to get the structural information, we have used the high-resolution data bank (150°). Since magnetic intensities are relatively weak compared to the nuclear peaks, we have used 60° bank where stronger signal can be obtained at the expense of resolution. In addition, large *d*-spacing diffraction data, where the effects of magnetic form factor are reduced, will significantly improve the analysis, and these data can be collected at the 60° bank. The highest *d* spacing achieved in 150°, 90°, and 60° banks are 3.96, 5.41, and 7.65 Å. Most of the data were analyzed using the General Structure Analysis System (GSAS) program.[10] The neutron coherent scattering lengths used for ^{248}Cm, Cu, and O in units of 10^{-12} cm are 0.77, 0.77, and 0.58, respectively.

RESULTS AND DISCUSSION

Atomic structure refinement

The room-temperature neutron-diffraction pattern is shown in Fig. 1. The relatively high background results from a combination of the very small sample size, the large incoherent scattering from the vanadium can, and the contribution of neutrons from the decay of ^{248}Cm. The latter has been previously demonstrated to contribute significantly to the measured background in experiments similar to those discussed herein.[11] Oscillations in the baseline arise from errors in background removal.

Although the Cm_2CuO_4 sample is single phase, it is necessary to include three phases in order to fully index all the observed lines in the powder pattern. In addition to the compound of interest, there are contributions from the vanadium of the sample holder and cadmium from the mask. Vanadium has only a very small coherent scattering cross section for neutrons therefore the Bragg peaks from this phase are very weak. Whereas the phase was included in the analysis, the phase was not refined. Cd, which has a larger scattering cross section was also included in the analysis, but the phase refined poorly. This is because Cd has a high absorption cross section, it was not in powder form and it was used as a mask, which means that it does not diffract from the scattering center.

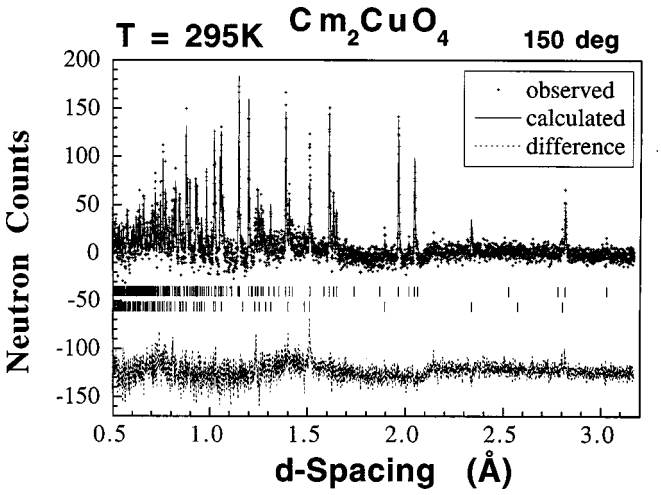

FIG. 1. Room-temperature diffraction pattern and refinement for Cm_2CuO_4. These data were collected for 24 h at an average diffraction angle of 150°. The crosses are the observed data, which are not normalized to the incident beam, and the solid line is the refinement. The difference between the observed and the refined structure is shown at the bottom. The two sets of vertical lines indicate the positions of nuclear Bragg peaks originating from Cm_2CuO_4 (top) and Cd (bottom).

The peaks in Fig. 1 that are attributed to Cm_2CuO_4 can be indexed with (h,k,l) with $h+k+l=$ even and assigned to the space group $I4/mmm$ (space group 139). This is the same space group that has been reported for the other R_2CuO_4 (R = Pr, Nd, Sm, Eu, and Gd).[12] The intensities of the neutron peaks in Fig. 1 confirm that Cm_2CuO_4 crystallizes in the T' phase, and is isostructural with the Pr-Gd[13] analogs. The crystallographic sites of the Cm, Cu, O(1), and O(2) in the $I4/mmm$ space group are $4e(0,0,z)$, $2a(0,0,0)$, $4c(0,0.5,0)$, and $4d(0,0.5,0.25)$. The calculated powder-diffraction pattern is compared to the room-temperature data as shown in Fig. 1. The lattice constants and structural parameters determined from the best fit are listed in Table I.

The neutron data collected at 35 and 15 K were also fitted to determine the atomic structure. There is no indication from these data of a structural phase change at lower temperature. The linewidths remain narrow at all temperatures, with no indication of any of the stacking faults or lower symmetry that has been seen in the structure or magnetic ordering of other high-T_c oxides.[14–17] The only observed change is the normal Debye-like thermal contraction of the lattice and a decrease in the isotropic thermal parameters with decreasing temperature.

TABLE I. Results of the structural refinements at room temperature (RT), 35 K, and 15 K. Lattice parameters (a and c), volume of a unit cell, the z of the Cm ion, and Cm-O distances (r_1 and r_2) are shown here. Cm has eight nearest-neighbor oxygen atoms: four at distance r_1 and other four at distance r_2. Note that the atomic position for Cm is $(0,0,z)$. The structure at 15 K was not refined because of the additional magnetic intensities present below 25 K.

Temperature	RT	35 K	15 K
a (Å)	3.9305(1)	3.9234(2)	3.9234(1)
c (Å)	12.1120(7)	12.0785(11)	12.0745(8)
Volume (Å)	187.120(11)	185.927(17)	185.860(14)
z	0.3511(4)	0.3510(5)	
r_1	2.3153(22)	2.3102(34)	
r_2	2.6676(29)	2.6624(40)	

A comparison of the lattice constants and R-O distances obtained here for the Cm compound with those observed for other trivalent R in R_2CuO_4 is consistent with the expectation that Cm is trivalent in this compound. For example, unit-cell volumes as a function of trivalent ionic radii are plotted in Fig. 2. The ionic radius of trivalent Cm (1.10 Å) is significantly larger than that of tetravalent Cm (0.95 Å).[18] The lattice parameters, unit-cell volume, and R-O distances for various R in R_2CuO_4 (Refs. 19 and 20) increases smoothly with increasing ionic radii, and Cm_2CuO_4 follows the same trend. The trivalent ionic radius of Cm is only slightly less than that of Nd, and the measured lattice parameters, volume, and R-O distances of Cm are also only slightly smaller than those of Nd. If the Cm ion was tetravalent, these values would be significantly smaller, therefore the neutron-diffraction data at all temperatures are consistent with trivalent Cm in Cm_2CuO_4. The Cu-O distances also follow the trends established for the other members of the T' series, and show no shortening that could explain either the high magnetic ordering temperature or the absence of superconductivity in the doped material. There is no evidence from our refinement of interstitial Cm or O in this compound.

X-ray-absorption near-edge spectroscopy

The L_3-edge absorption spectrum from Cm in Cm_2CuO_4 is compared with similar spectra taken on trivalent and tetravalent standards in Fig. 3. The spectrum from the Cm^{3+} has a maximum at 18 979 eV. The absorption-edge position, as defined by the peak in the first derivative (shown in the figure inset) is at 18 973 eV. The Cm^{4+} standard has a maximum at 18 984 eV with an absorption-edge position of 18 977 eV. The 4-eV shift of edge position to higher energy with increasing Cm valence is consistent with shifts observed for 3+/4+ spectra from other actinide ions.[18,21,22] X-ray absorption near-edge structure XANES data on Cm_2CuO_4 have a peak at about 18 979 eV with an absorption edge at 18 973 eV. A comparison between the data from Cm_2CuO_4 and the valence standards demonstrates that Cm is trivalent in Cm_2CuO_4. An analysis of L_2- and L_1-edge data (not shown) provide the same result. Our measured L_2 and L_1 Cm edges are at 23 662 and 24 547 eV for the standard and our CuO sample whereas these same edges were at 23 666 and 24 551 eV for tetravalent Cm in CmO_2. It should be noted that these measured edge energies are significantly different from those tabulated in the literature.[8] There is no evidence of Cm^{4+} in Cm_2CuO_4. The XANES results, together with the neutron-diffraction analysis, show that Cm is trivalent.

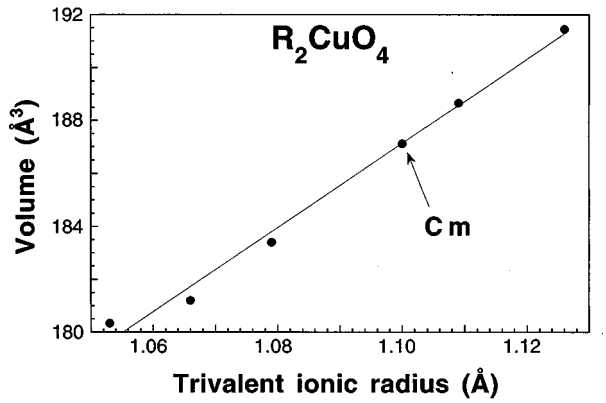

FIG. 2. Unit-cell volume of R_2CuO_4 as a function of trivalent (R^{3+}) ionic radius for various R. Volumes for other R, and trivalent ionic radii were obtained from elsewhere (Refs. 18 and 19).

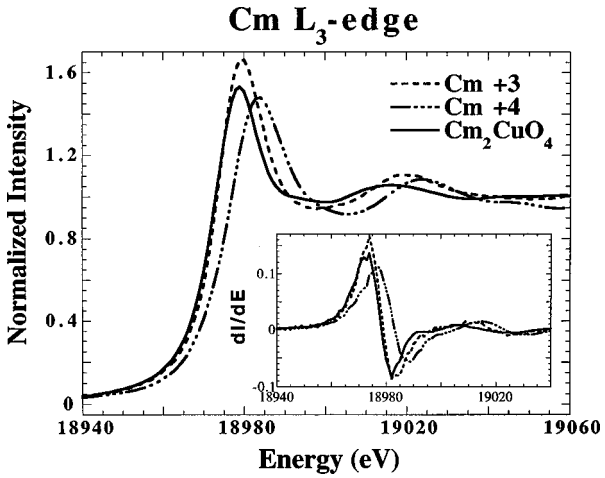

FIG. 3. The Cm L_3-edge XANES spectra for Cm_2CuO_4 is compared to a spectrum obtained from trivalent (solution) and tetravalent (CmO_2) Cm standards. The fluorescence data are shown for Cm solution, whereas transmission data are shown for CmO_2 and Cm_2CuO_4 because the thickness of the sample may vitiate the florescence data. However florescence spectra also qualitatively show the same results. The inset shows the first derivative of the intensities. The similarity between the two spectra obtained from Cm solution and Cm_2CuO_4 indicates that Cm ions are in the trivalent state in Cm_2CuO_4. There is no evidence of a tetravalent component to the spectrum.

Magnetic susceptibility

The magnetic susceptibility of Cm_2CuO_4 as a function of temperature is shown in Fig. 4.[3] Fitting the data above 50 K to $\chi = c/(T+\theta)$ demonstrates Curie Weiss behavior. The effective moment μ_{eff}, determined from the Curie constant $c[\mu_{\text{eff}} = (8c)^{1/2}]$, is $7.89(5)\mu_B$. The measured effective moment is expected to be dominated by Cm^{3+}, which has a free-ion magnetic moment of $7.94\mu_B$. In contrast, the spin only moment expected for Cu^{2+} is $1.73\mu_B$. The Cm to Cu

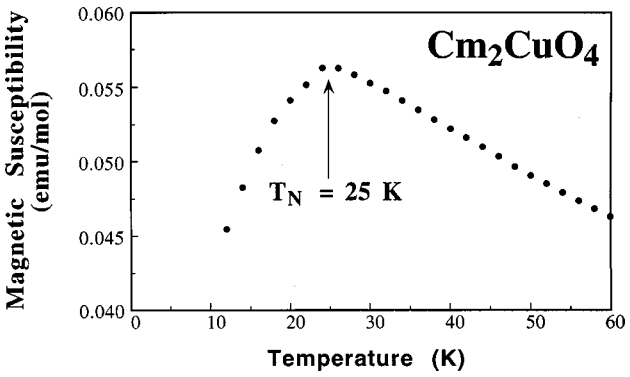

FIG. 4. The temperature dependence of the magnetic susceptibility for Cm_2CuO_4 at low temperatures.[3] The cusp at 25 K indicates the antiferromagnetic ordering of Cm ions in this compound.

ration is 2:1, and the measured susceptibility is proportional to the square of the effective moment, therefore no direct information can be determined from the measured susceptibility about the magnetic behavior of Cu in this compound. Any splitting of the $^8S_{7/2}$ ground state is not expected to significantly influence the magnetic susceptibility over the temperature range used to determine the effective moment.

The effective moment determined here for Cm_2CuO_4 is the same as that determined for the trivalent sesquioxide Cm_2O_3,[23] but smaller than the $8.9(3)\mu_B$ determined for $CmBa_2Cu_3O_7$,[24] and larger than the 7.64 μ_B determined for $Cs_2NaCmCl_6$.[25] It is clear from these measurements that Cm^{3+} has an effective moment near to that expected from Russell Saunders coupling. This result is not consistent with a previous calculation that suggests intermediate coupling will significantly reduce the magnetic moment of Cm^{3+} at higher temperature.[25] Finally, it should be noted that Cm^{4+} has a $^7F_0$ ground term and therefore an effective moment of $0\mu_B$ at lower temperatures. The presence Cm^{4+} would result in a measured susceptibility reduced from the free-ion value. The fact that our measurement is in agreement with expectation for Cm^{3+} supports our conclusions based on the structural and XANES data.

The low-temperature magnetic susceptibility as a function of temperature, also shown in Fig. 4, has a cusp centered at 25 K. The magnitude of the cusp indicates that it arises from the ordering of Cm moments. Although this type of cusp behavior is expected for antiferromagnetic ordering, it could also result from a splitting of the Cm^{3+} ground state, as mentioned above. In order to determine if the observed cusp is a result of an ordering of the Cm^{3+} moments, low-temperature neutron-diffraction data were obtained and analyzed for a contribution from coherent magnetic scattering.

Magnetic structure

A comparison of the neutron-diffraction data obtained at room temperature, 35 K, and 15 K shows no indication of additional peaks or line broadening at lower temperatures. This observation rules out both a structural phase change and new peaks arising from magnetic ordering of the Cm moments. In order to further probe for any magnetic contribution to the 15-K data, which is below the cusp temperature, we directly compare the intensities of the 35 and 15 K data in Fig. 5. At 35 K, the data are adequately modeled assuming

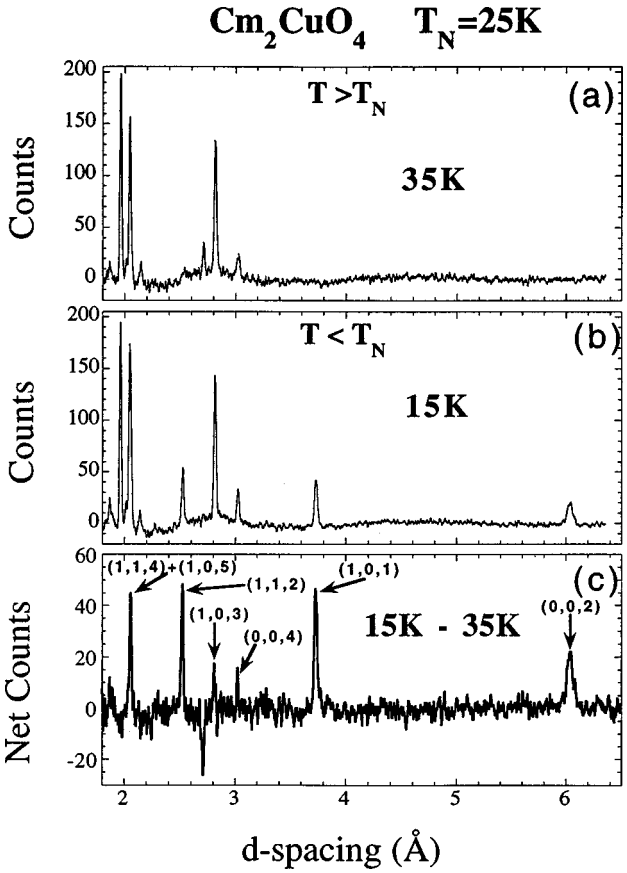

FIG. 5. Neutron powder diffraction pattern for Cm_2CuO_4, which has T_N of 25 K. These data, which are not normalized to the incident beam, were collected at an average diffraction angle of 60 degree. (a) data at 35 K (above T_N) where only nuclear peaks are observed. (b) At 15 K (below T_N) where both nuclear and magnetic peaks are observed. (c) Magnetic diffraction pattern obtained by subtracting the 35-K data from the data at 15 K. Both nuclear and magnetic peaks appear at the same position.

only nuclear contributions to the intensities. At 15 K some of the Bragg peaks show markedly increased intensities that are attributed to diffraction from ordered Cm moments. This increased intensity can be seen from the diffraction pattern shown in Fig. 5(c), which was obtained by subtracting the 35-K data from the 15-K data.

All observed magnetic peaks shown in Fig. 5(c) coincide with nuclear peaks. They can be indexed as (h,k,l) based on the chemical unit cell, where all h, k, l are integers with $h+k+l=$even. The chemical and magnetic unit cells in Cm_2CuO_4 are the same and the propagation vector is (0,0,0). Precedents for this magnetic symmetry are seen in Sm_2CuO_4 (Ref. 26) and Gd_2CuO_4,[27] in which all magnetic peaks from R ordering coincide with nuclear peaks. The absence of $(h/2,k/2,l)$-type peaks, where both h and k are odd, eliminates the possibility of a simple antiferromagnetic ordering in the a-b plane like the one observed for Nd in Nd_2CuO_4.[28,29] The well defined magnetic peaks in the difference spectrum confirm the hypothesis that the cusp in the susceptibility arises from an ordering of magnetic moments, and not from a structural phase change or from crystal-field effects.

The nature of the magnetic ordering in Cm_2CuO_4 can be determined from the data shown in Fig. 5(c) after they are

TABLE II. Observed and calculated intensities (square of magnetic structure factors) of the magnetic Bragg intensities from Cm_2CuO_4 at 15 K. The observed intensities were normalized to the incident beam and corrected for multiplicity factor (M_τ) and the Lorentz factor (L_τ).

Peak position (d) in Å	Indexing	Multiplicity (M_τ)	Observed intensity	Calculated intensity
6.038	(0,0,2)	2	20.3±3.0	20.5
3.734	(1,0,1)	8	5.8±0.7	6.1
3.023	(0,0,4)	2	1.7±2.0	4.3
2.814	(1,0,3)	8	0.8±0.5	1.0
2.524	(1,1,2)	8	6.6±1.2	5.6
2.047	(1,0,5)	8	9.4±2.6	8.5
	(1,1,4)	8		
1.869	(2,0,2)	8	4.3±1.4	2.4

corrected for the incident neutron flux, which varies with d spacing. The magnetic diffraction intensities are proportional to the square of the magnetic moment, and for a simple collinear magnetic structure are given by[30]

$$I_\tau = C\left[\frac{\gamma e^2}{2mc^2}\right]^2 \langle\mu\rangle^2 [f(\tau)]^2 |F_M|^2 \langle 1-(\hat{\tau}\cdot\hat{\mu})^2\rangle M_\tau L_\tau . \qquad (1)$$

Here C is an instrument constant, which is obtained using the intensities of the nuclear peaks. The quantity in the large parentheses is the neutron electron coupling constant (-0.27×10^{-12} cm), $\langle\mu\rangle$ is the thermal average of the ordered moment, and $f(\tau)$ is the magnetic form factor. The magnetic form factor for Cm has been previously calculated by Desclaux and Freeman.[31] M_τ is the multiplicity factor for powder reflection, L_τ is Lorentz factor, and F_M is the magnetic structure factor. $\hat{\tau}$ and $\hat{\mu}$ are unit vectors in the direction of the reciprocal-lattice vector τ and the moment direction, with an orientation factor $\langle 1-(\hat{\tau}\cdot\hat{\mu})^2\rangle$ that must be calculated for all possible domains.

The intensities of the observed peaks, after corrections for incident beam intensity, Lorentz factor and multiplicities, are listed in Table II. The strongest peak is the (0,0,2) reflection. Note that this peak, together with (1,0,1), has a negligible nuclear contribution to its intensity, as shown in Fig. 5(a), and hence the magnetic contribution to these peaks are easily observable. The observation of an intense (0,0,2) reflection rules out the possibility that the magnetic moment orders along the c axis. If the moment were to order along the c axis, then the reciprocal lattice vector τ and the moment direction μ would be parallel, and the $(0,0,l)$ reflections would have zero intensity. Such a structure is observed for Sm_2CuO_4.[26] The observation of a strong (0,0,2) reflection shows that the moments order in the a-b plane. The easy direction within the a-b plane of a tetragonal structure cannot be obtained from domain-averaged, powder neutron data.[32]

The magnitude of the magnetic peak intensities listed in Table II indicates that the Cm must be involved in the transition at 25 K. The observed magnetic intensities are too strong to be explained in terms of Cu moment ordering. Assuming a Cm form factor, we obtained $4.8(2)\mu_B$ for the ordered moment of Cm at 15 K. This moment is smaller than

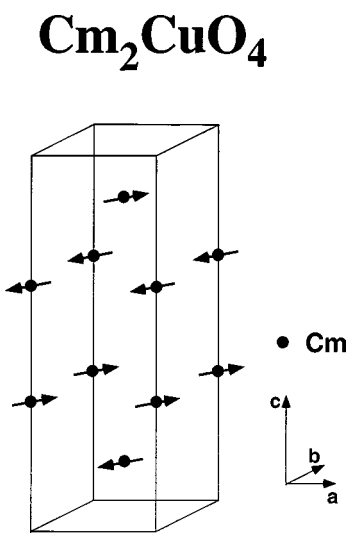

FIG. 6. Cm magnetic structure in Cm_2CuO_4. The spins in the a-b planes are aligned parallel, while the spins in the adjacent planes are aligned antiparallel. The spin direction is in the a-b plane. The specific direction within the a-b plane cannot be obtained from our powder-diffraction data.

expected for an f^7 configuration assuming a simple Russell-Saunders coupling scheme. The full saturation moment for the spherically symmetric ground state is expected to be $7\mu_B$. The reduced value obtained for the ordered moment may be the result of a splitting of the Cm^{3+} ground state.[7] However, it is probable that the temperature is not low enough to have measured the full saturation moment. If the Cm-moment ordering follows a Brillouin function, the reduced moment of $4.8(2)\mu_B$ would correspond to a temperature of about 19 K. A similar temperature is obtained if it is assumed that the reduced moment follows the same temperature dependence as that previously determined for Gd in Gd_2CuO_4.[26] This temperature is within our rather large experimental error, which arises because of the extensive sample containment and the self-heating from ^{248}Cm radioactive decay. Therefore the somewhat reduced moment determined from Cm in Cm_2CuO_4 can be rationalized without the necessity to invoke any crystal-field effects. The observed and calculated intensities are given for selected magnetic peaks in Table II.

The Cm spins in Cm_2CuO_4 have the simple magnetic structure shown in Fig. 6. This structure consists of ferromagnetic sheets (spins aligned parallel) in the a-b plane, with spins in adjacent sheets along the c axis coupled antiferromagnetically. This structure is the same as that previously observed for Gd, which is the $4f$ counterpart of Cm, in Gd_2CuO_4.[27]

There is no evidence of Cu moment ordering in our neutron-diffraction data. The ordered moment of Cu is expected to be small ($\sim0.2-0.5\mu_B$). Our very small sample size (42 mg) and the contribution to the neutron background from ^{248}Cm radioactive decay combine to render unobservable a contribution from such a small moment. Unfortunately, information about the Cu moment ordering is necessary for understanding the overall effect that magnetism has on superconductivity in the Th-doped sample. On the one hand, without direct evidence to the contrary, it could be

argued that the Cu sublattice in Cm_2CuO_4 behaves similarly to that for all other R_2CuO_4. Cu moments in these materials order at similar temperatures, near room temperature, and with similar antiferromagnetic structures.[12] On the other hand, perhaps the Cm moments have strong enough interactions to influence the Cu ordering. Precedence for this influence is found in the Pr-Gd analogs, in which R appears to influence details of copper ordering.[12] The Cm moments order at 25 K, which is a much higher temperature than the 5.95 K found for Sm_2CuO_4 (Ref. 33) or the 6.5 K found for Gd_2CuO_4.[34] Even with appropriate doping of Th, the Cm compound has a cusp in the susceptibility at 13 K, indicating the Cm moment ordering persists at doping levels that are expected to result in superconductivity.

In the rare-earth cuprates, nearest-neighbor Cu spins in the a-b plane order antiferromagnetically. In particular, there is a strong coupling between the Nd and Cu sublattices in Nd_2CuO_4 because the Nd and Cu have the same magnetic symmetry.[28,35] In Pr_2CuO_4 the Cu sublattice induces a small moment on Pr^{3+},[29] which has a singlet ground state in this material.[36] The antiferromagnetically ordered Cu sublattice produces a net polarizing field at the R site. This field has the same symmetry as the Nd magnetic symmetry when it orders spontaneously. The induced moment for Nd was observed to temperatures as high as 80 K as the result of this polarizing field. Such a strong coupling is not observed in Sm_2CuO_4 or Gd_2CuO_4 because the rare-earth and Cu magnetic structures are different. It is expected that the Cm and Cu magnetic structures are different from each other in Cm_2CuO_4 also, and such a strong coupling is not expected. In principle, the Cu sublattice polarizes rare-earth spins in all R_2CuO_4 compounds, and there is an indication for an induced Gd moment due to the polarization by the Cu sublattice in Gd_2CuO_4.[37] Such a small effect cannot be ruled out from our neutron measurements, which were obtained on a powder sample.

It is expected that exchange interactions are responsible for the Cm moment ordering in this system. Clearly dipole interactions can be ruled out because the maximum temperature expected for dipole-type ordering is less than about 2 K. The Cm ordering temperature (T_N) is higher than any other R ordering temperature in R_2CuO_4, where highest T_N observed is 6.4 K for Gd.[34] The unusually high ordering temperature in Cm_2CuO_4 indicates that the exchange interactions are very strong in this compound.

Cm_2CuO_4 does not superconduct when appropriately doped with electrons,[3] in contrast to all the other T' R_2CuO_4 compounds, except Gd. There is no anomaly in their structures that could suggest a reason for this behavior. It has been previously suggested that the Gd analog does not superconduct because the solid solution range of $Gd_{2-x}Ce_xCuO_4$ does not extend to high enough x to introduce sufficient carriers. This argument does not appear valid for the Cm analog. X-ray diffraction on the Th-doped Cm sample shows no evidence of phase separation. The most probably impurity phase is ThO_2. Its high symmetry and its stoichiometry, together with the high atomic number of Th, indicate that ThO_2 should be detectable, even at low concentrations in the sample.

Cm_2CuO_4 and Gd_2CuO_4 have two other features in common. They both have an f^7 configuration and therefore a spherically symmetric ground state, to first order. It has been previously suggested that the lack of an orbital contribution to the ground state inhibits superconductivity.[38] This argument is difficult to rationalize with the results obtained herein, in part because the Cm ground state is known to split, as the result of intermediate coupling,[7] with an overall splitting in the energy range that could significantly influence superconductivity and magnetic ordering. The other feature that they have in common is their high magnetic ordering temperatures relative to other R_2CuO_4. In part this may be due to the large moment on Gd and Cm. However, it should be stressed that high magnetic ordering temperatures are also observed for $PrBa_2Cu_3O_7$ and $CmBa_2Cu_3O_7$, which also do not superconduct. In addition, $Pb_2Sr_2Pr_{1-x}Ca_xCu_3O_8$ shows a modestly elevated $T_N(x=0)$ for Pr ordering, at the same time it has a modestly reduced $T_c(x=.5)$. Gd and Cm in the R_2CuO_4 series have the same magnetic structure to their ordered moments, and this structure is different from the other analogs of this series that are the parent phases of the electron superconductors. Therefore it is important to understand as much as we can about the magnetic behaviors of these compounds. Unfortunately, we were not able to determine information about the Cu moment ordering from these experiments, which might prove useful in understanding the role of symmetry and magnetism in the high-T_c cuprates.

ACKNOWLEDGMENTS

We would like to thank G. H. Lander and J. W. Richardson for helpful discussions. Work at Argonne is supported by the DOE Basic Energy Sciences, Chemical Sciences, under W-31-109-ENG-38.

[1] J. G. Bednorz and K. A. Muller, Z. Phys. B **64**, 189 (1986).
[2] H. Takagi, S. Uchida, and T. Tokura, Phys. Rev. Lett. **62**, 1197 (1989).
[3] L. Soderholm, C. W. Williams, and U. Welp, Physica C **179**, 440 (1991).
[4] H. A. Blackstead and J. D. Dow, Phys. Rev. B **55**, 6605 (1997).
[5] L. Soderholm and C. W. Williams, in *Physical and Material Properties of High Temperature Superconductors*, edited by S. K. Malik and S. S. Shah (Nova Science Publishers, New York, 1992), pp. 59–76.
[6] P. G. Eller and R. A. Penneman, in *The Chemistry of the Actinide Elements*, edited by J. J. Katz, G. T. Seaborg, and L. R. Morss (Chapman and Hall, London, 1986), Vol. 2, pp. 962–988.
[7] G. K. Liu, J. V. Beitz, and J. Huang, J. Chem. Phys. **99**, 3304 (1993).
[8] J. A. Bearden and A. F. Burr, Rev. Mod. Phys. **39**, 125 (1967).
[9] F. W. Lytle, in *Applications of Synchrotron Radiation*, edited by H. Winick, D. Xian, M. H. Ye, and T. Huang (Gordan and Breach, New York, 1989), Vol. 4, p. 135.
[10] A. C. Larson and R. B. V. Dreele, Los Alamos National Laboratory Report No. LAUR-86-748, 1990 (unpublished).
[11] L. R. Morss, J. W. Richardson, C. W. Williams, G. H. Lander, A.

C. Lawson, N. M. Edelstein, and G. V. Shalimoff, J. Less-Common Met. **156**, 273 (1989).
[12] J. W. Lynn and S. Skanthakumar, in *Handbook on the Physics and Chemistry of Rare Earths*, edited by J. K. A. Gschneidner, L. Eyring, and M. B. Maple (Elsevier Science, New York, 1999).
[13] H. Muller-Buschbaum and W. Wollschlager, Z. Anorg. Allg. Chem. **414**, 76 (1975).
[14] B. Roessli, P. Fischer, U. Staub, M. Zolliker, and A. Furrer, Europhys. Lett. **23**, 511 (1993).
[15] T. W. Clinton, J. W. Lynn, J. Z. Liu, Y. X. Jia, T. J. Goodwin, R. N. Shelton, B. W. Lee, M. Buchgeister, M. B. Maple, and J. L. Peng, Phys. Rev. B **51**, 15 429 (1995).
[16] U. Staub, L. Soderholm, S. Skanthakumar, S. Rosenkranz, C. Ritter, and W. Kagunya, Z. Phys. B **104**, 37 (1997).
[17] U. Staub, L. Soderholm, S. Skanthakumar, P. Pattison, and K. Conder, Phys. Rev. B **57**, 5535 (1998).
[18] L. Soderholm, C. Williams, S. Skanthakumar, M. R. Antonio, and S. Conradson, Z. Phys. B **101**, 539 (1996).
[19] R.-C. Shen, T.-Q. Tyan, T.-H. Meen, and H.-D. Yang, Jpn. J. Appl. Phys., Part 1 **34**, 1839 (1995).
[20] C.-K. Loong and L. Soderholm (private communications).
[21] G. Kalkowski, G. Kaindl, S. Bertram, G. Schmiester, J. Rebizant, J. C. Spirlet, and O. Vogt, Solid State Commun. **64**, 193 (1987).
[22] L. Soderholm, M. R. Antonio, C. W. Williams, and S. R. Wasserman (unpublished).
[23] L. R. Morss, J. Fuger, J. Goffart, and R. G. Haire, Inorg. Chem. **22**, 1993 (1983).
[24] L. Soderholm, G. L. Goodman, U. Welp, C. W. Williams, and J. Bolender, Physica C **161**, 252 (1989).
[25] M. E. Hendricks, E. R. Jones, J. A. Stone, and D. G. Karraker, J. Chem. Phys. **60**, 2095 (1974).
[26] I. W. Sumarlin, S. Skanthakumar, J. W. Lynn, J. L. Peng, W. Jiang, Z. Y. Li, and R. L. Greene, Phys. Rev. Lett. **68**, 2228 (1992).
[27] T. Chattopadhyay, P. J. Brown, A. A. Stepanov, P. Wyder, J. Voiron, A. I. Zvyagin, S. N. Barilo, D. I. Zhigunov, and I. Zobkalo, Phys. Rev. B **44**, 9486 (1991).
[28] J. W. Lynn, I. W. Sumarlin, S. Skanthakumar, W.-H. Li, R. N. Shelton, J. L. Peng, Z. Fisk, and S.-W. Cheong, Phys. Rev. B **41**, R2569 (1990).
[29] M. Matsuda, K. Yamada, K. Kakurai, H. Kadowaki, T. R. Thurston, Y. Endoh, Y. Hidaka, R. J. Birgeneau, M. A. Kastner, P. M. Gehring, A. H. Moudden, and G. Shirane, Phys. Rev. B **42**, 10 098 (1990).
[30] G. E. Bacon, *Neutron Diffraction* (Oxford University Press, Oxford, 1975).
[31] J. P. Desclaux and A. J. Freeman, in *Handbook on the Physics and Chemistry of the Actinides*, edited by A. J. Freeman and G. H. Lander (North-Holland, Amsterdam, 1984), Vol. 1, pp. 1–77.
[32] G. Shirane, Acta Crystallogr. **12**, 282 (1959).
[33] M. F. Hundley, J. D. Thompson, S. W. Cheong, Z. Fisk, and S. B. Oseroff, Physica C **158**, 102 (1989).
[34] J. D. Thompson, S.-W. Cheong, S. E. Brown, Z. Fisk, S. B. Oseroff, M. Tovar, D. C. Vier, and S. Schultz, Phys. Rev. B **39**, 6660 (1989).
[35] S. Skanthakumar, J. W. Lynn, J. L. Peng, and Z. Y. Li, J. Magn. Magn. Mater. **104–107**, 519 (1992).
[36] C. K. Loong and L. Soderholm, Phys. Rev. B **48**, 14 001 (1993).
[37] T. Chattopadhyay, P. J. Brown, and B. Roessli, J. Appl. Phys. **75**, 6816 (1994).
[38] H. A. Blackstead, J. D. Dow, A. K. Heilman, and D. B. Pulling, Solid State Commun. **103**, 581 (1997).